

Capacitance transient study of a bistable deep level in e(-)-irradiated n-type 4H-SiC

Franziska Beyer, Carl Hemmingsson, Henrik Pedersen, Anne Henry, J Isoya, N Morishita, T Ohshima and Erik Janzén

Linköping University Post Print

N.B.: When citing this work, cite the original article.

Original Publication:

Franziska Beyer, Carl Hemmingsson, Henrik Pedersen, Anne Henry, J Isoya, N Morishita, T Ohshima and Erik Janzén, Capacitance transient study of a bistable deep level in e(-)-irradiated n-type 4H-SiC, 2012, Journal of Physics D: Applied Physics, (45), 45.

<http://dx.doi.org/10.1088/0022-3727/45/45/455301>

Copyright: Institute of Physics

<http://www.iop.org/>

Postprint available at: Linköping University Electronic Press

<http://urn.kb.se/resolve?urn=urn:nbn:se:liu:diva-85846>

Capacitance transient study of a bistable deep level in e⁻-irradiated n-type 4H-SiC

F. C. Beyer^{1‡}, C. G. Hemmingsson¹, H. Pedersen¹, A. Henry¹,
J. Isoya², N. Morishita³, T. Ohshima² and E. Janzén¹

¹ Department of Physics, Chemistry and Biology, Linköping University, SE-581 83 Linköping, Sweden

² Graduate School of Library, Information and Media Studies, University of Tsukuba, Tsukuba, Ibaraki 305-8550, Japan

³ Japan Atomic Energy Agency, 1233 Watanuki, Takasaki, Gunma 370-1292, Japan

E-mail: fbeyer@ifm.liu.se

Abstract. Using capacitance transient techniques, a bistable center, here called FB-center, was observed in electron irradiated 4H-SiC. In configuration A, the deep level known as EH5 ($E_a = E_C - 1.07$ eV) is detected in the deep level transient spectroscopy spectrum, whereas for configuration B no obvious deep level is observed in the accessible part of the band gap. Isochronal annealing revealed the transition temperatures to be $T_{A \rightarrow B} > 730$ K and for the opposite process $T_{B \rightarrow A} \approx 710$ K. The energy needed to conduct the transformations were determined to $E_A(A \rightarrow B) = (2.1 \pm 0.1)$ eV and $E_A(B \rightarrow A) = (2.3 \pm 0.1)$ eV, respectively. The pre-factor indicated an atomic jump process for the opposite transition $A \rightarrow B$ and a charge carrier-emission dominated process in case of $B \rightarrow A$. Minority charge carrier injection enhanced the transformation from configuration B to configuration A by lowering the transition barrier by about 1.4 eV. Since the bistable FB-center is already present after low-energy electron irradiation (200 keV), it is likely related to carbon.

PACS numbers: 78.70.-g, 73.50.Gr

Submitted to: *J. Phys. D: Appl. Phys.*

1. Introduction:

Some defects in semiconductors show an unstable behavior depending on the existing electronic, thermal and/or optical environment [1]. One charge state may exist in different configuration states, which are separated by energy barriers. Depending on the initial thermal, optical and electronic conditions, one of the configurations will be stable. Changing the conditions by adding thermal or optical energy, the energy barrier can be surmounted and the defect transforms to another configuration. If only

‡ current adress: Institute for Applied Physics, TU Bergakademie Freiberg, Leipziger Straße 23, D-09596 Freiberg, Germany

two configurations are available, the defect is called bistable, otherwise multistable [2]. Commonly, such kinds of defects are called metastable, since for instance capacitance investigations show a metastable character; levels in the band gap will be filled or emptied depending on the initial conditions. Depletion regions formed in junction devices such as pn- or Schottky diodes are suitable for studying metastable defects, since the defects can be occupied or unoccupied with charge carriers. Depending on the depletion region width, i.e. the applied voltage and the shallow doping concentration, the defects will be located below or above the Fermi level and thus will be filled or emptied, respectively. Deep level transient spectroscopy (DLTS) combined with bias on/off cycles is a suitable tool to investigate metastable defects. During device operation, thermal and electronic conditions may vary and thus inherent defects may change their behavior. Thus it is important to study such transformation processes and their transition conditions.

Metastable defects have been extensively studied for years in Si [3–7], GaAs [8, 9] and InP [10, 11]. Recently, several bistable [12–15] and multistable [16] defects have also been reported in the SiC for its polytypes 4H- and 6H-SiC, respectively. In 6H-SiC, Hemmingsson et al. [16] investigated a metastable defect with three different configurations.

Electron irradiation is used to introduce intrinsic defects and by varying the irradiation energy tentative identification of the generated defect can be achieved. The displacement energy of silicon atoms in SiC is higher than that of carbon. If the irradiation energy, E_{irr} is less than the energy needed for moving the Si in SiC ($E_{irr} < 220$ keV [17]), the introduced defects are likely related to C interstitials or C vacancies. There have been several investigations on both high-energy irradiated [18–23] and low-energy irradiated [24–26] SiC. In a recent study [15], we discussed the annealing of EH1, EH3 and the bistable M-center, which was discovered and labelled by Martin et al. [12], as well as the related formation of the bistable EB-centers in low-energy irradiated SiC, which were discovered and labelled by Beyer et al. [14]. Finally, the annihilation of the EB-centers at about 700 °C and their association with carbon interstitials and/or related complexes were reported. The deep level EH5 related to a defect introduced after low-energy electron irradiation, has not been studied in detail.

In this study, we investigate the bistable behavior of a defect, labeled FB-center, in 4H-SiC, which gives rise to band gap states associated with the known deep level EH5. The defect has two configurations A and B (see configuration coordination (CC) diagram in Figure 1), which can be transformed into each other thermally and/or optically. Under zero-bias condition during high-temperature annealing, the defects capture electrons. The thermal energy is sufficient for the transition from configuration $A \rightarrow B$ ($E_A(A \rightarrow B) = 2.1$ eV). The defects are stable in configuration B only if they are occupied by an electron, B^{n-1} . If at such temperatures, the reverse bias is increased to V_r , the defects will transform from configuration $B \rightarrow A$ ($E_A(B \rightarrow A) = 2.3$ eV). Since the thermal energy is higher than the electron ionization energy, the defects will directly emit their electrons and thus be stabilized in $A^n + e^-$. Keeping the bias stable at V_r

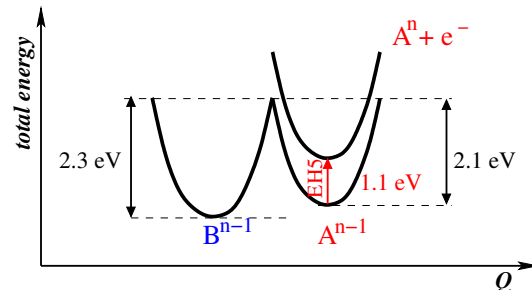


Figure 1. (Color online) Suggested configuration coordinate diagram for the FB-center in electron irradiated 4H-SiC.

during cooling to the DLTS starting temperature, the DLTS peak EH5 will be detected in the subsequent DLTS measurement as electron emission from configuration A after electron capture during the DLTS filling pulse ($A^n + e^- \rightarrow A^{n-1}$). The FB-center in configuration A is often observed both after low- and high-energy electron irradiation as the DLTS peak EH5 in 4H-SiC, which suggests a carbon related defect as its origin.

2. Experimental procedure:

Capacitance investigations were performed on two types of samples. The first ones, were p^+n junctions, which were homoepitaxially grown by a standard chemical vapor deposition (CVD) process on highly doped 4H-SiC substrates. The high quality p^+ layer was achieved by Al-doping above 10^{18} cm^{-3} whereas the investigated n -layer had only a low ($\approx 10^{15} \text{ cm}^{-3}$) nitrogen doping concentration. Mesa structures were processed by reactive ion etching. The fabricated p^+n junctions were further irradiated by high-energy electrons (2.5 MeV) with a dose of $1 \times 10^{15} \text{ cm}^2$ at room temperature. The other type of samples were Schottky diodes, for which the unintentionally n -type doped layers were grown by a chloride-based CVD process on highly doped 4H-SiC substrates. The layers were irradiated by low-energy electrons (200 keV) with a dose of $5 \times 10^{16} \text{ cm}^2$ at room temperature. Thermally deposited Nickel (thickness about 1000 Å) onto the epilayer served as Schottky contact, whereas conductive silver paint formed the ohmic contact to the low resistive substrate. Capacitance-voltage (CV) measurements at room temperature revealed homogeneous net doping concentrations, $N_d - N_a$, of $3 \times 10^{15} \text{ cm}^{-3}$ for the p^+n junctions and $1 - 2 \times 10^{15} \text{ cm}^{-3}$ for the Schottky diodes, respectively. DLTS measurements were performed between 100 and 700 K with temperature ramps between 3.7 and 7.4 K/min, a steady reverse bias of 10 V, a filling pulse height of 10 V and width of 10 ms, if not mentioned differently. Minority charge carrier injection was realized by forward biasing the p^+n junctions or in case of Schottky diodes by light pulses with a multiline Ar-ion laser ($E_{laser} \gg E_g(4\text{H-SiC})$) to generate electron-hole pairs, respectively. A light spot larger than the Schottky diode area was used, since the contacts were not semitransparent. Thus electron-hole pairs generated within the diffusion length from the contact can diffuse into the investigated

area. The reconfiguration behavior was studied by annealing, which was done directly in the DLTS setup with the possibility to apply bias to the diodes, thus setting the defects in different configurations under the heat treatments. The defect concentrations, N_t , were determined from the DLTS peak amplitudes if $N_t \ll N_d - N_a$. Defects were prepared initially in different configurations, which enables obtaining the exact N_t by subtracting DLTS spectra. The reconfiguration temperature was determined by isochronal annealing; i.e. the annealing temperature was increased while the annealing time was kept constant. The reconfigurations rates were obtained by isothermal annealing; i.e. the annealing time was increased at various distinct temperatures. The two configurations A and B were achieved by stabilizing the defects with and without bias, respectively, above 700 K, followed by a fast cooling to the measurement starting temperature. Pulse train measurements (measurement of DLTS amplitudes as a function of the number of filling pulses) were performed at 500 K in order to investigate the transformation process from configuration B to A or the opposite transition.

3. Results and discussion:

Figure 2 shows DLTS spectra of the two configurations for a high- (a) and a low- (b) energy electron irradiated sample, respectively. The time window was 5 s^{-1} for (a) and (b). Common features were detected in the differently irradiated samples, such as the well-known $Z_{1/2}$ [[27]] and EH6/7 [[18]] levels. As reported by Storasta et al. [24], the EH6 level is more pronounced after high-energy irradiation, whereas after low-energy irradiation the EH6 smears out in the low temperature side of the asymmetric EH6/7 peak.

Additional to these prominent levels, EH4 is detected after high-energy irradiation but absent after low-energy irradiation, as reported previously by Alfieri et al. [22]; the authors attributed the defect to a complex defect or cluster of first-order defects.

3.1. DLTS peak EH5 in electron irradiated n -type $4H$ -SiC

The EH5 peak is seen in all spectra in both low- and high-energy irradiated samples. The electrical properties of all the defects are summarized in table 1. The curves labeled *mainly configuration B* in Figure 2 were obtained for samples prepared in configuration B^{n-1} by filling with electrons at $T \approx 730 \text{ K}$ (i.e. annealing without applied bias to the sample). If the annealing at the same temperature is done under a reverse bias of 10 V, the thermal energy is enough to surmount the barrier $B^{n-1} \rightarrow A^{n-1}$ and due to the absence of free electrons, the defects will stay in the unoccupied $A^n + e^-$ state, as seen from the CC diagram in Figure 1. Keeping the chosen bias condition and cooling down the sample, the defects capture an electron (A^{n-1}) during the DLTS filling pulses in the subsequent DLTS measurement, labeled *configuration A* in Figure 2. Electron emission occurs, if the thermal energy equals the ionization energy, which is observed as the EH5 peak. For the low-energy electron irradiated sample, a third

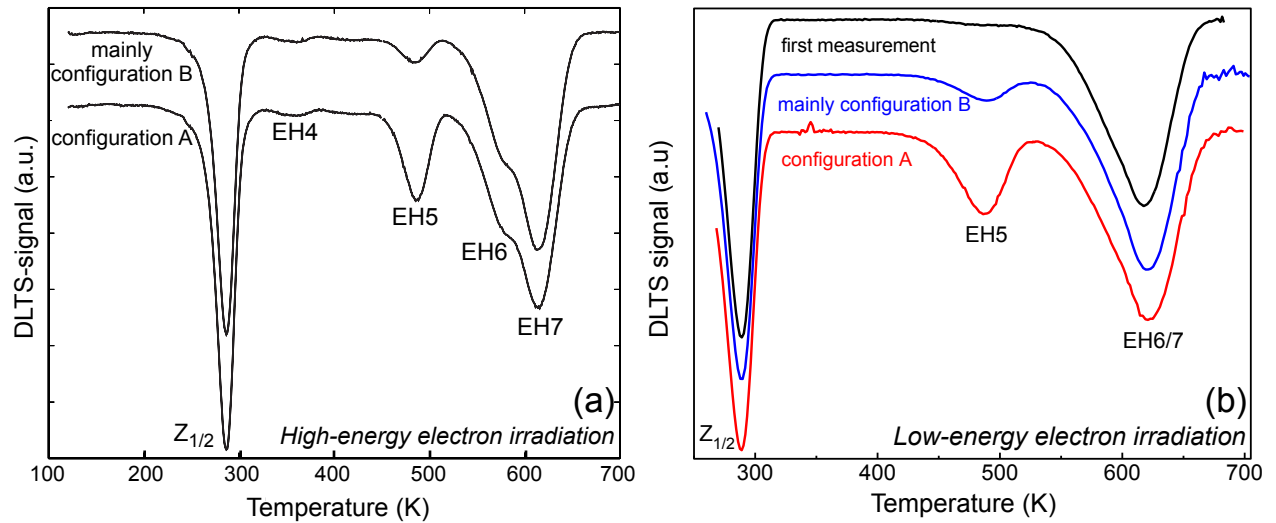


Figure 2. (Color online) DLTS spectra for high- (a) and low- (b) energy electron irradiated 4H-SiC. The defects were prepared in both configurations of the FB-center: initially in configuration B or initially in configuration A. Additionally, one DLTS spectrum direct after Schottky diode deposition, labeled first measurement is shown for the low-energy irradiated samples.

Table 1. Properties of the intrinsic levels in low-energy electron irradiated 4H-SiC: E_a and σ are obtained from Arrhenius plots ($\ln(e/T^2)$ versus $1000/T$), whereas σ_{meas} from DLTS measurements with different pulse length and N_t from the DLTS peak amplitudes, taking the two electron emission from the $Z_{1/2}$ level into account.

irradiation energy	peak	E_a (eV)	σ (cm ²)	σ_{meas} (cm ²)	N_t (cm ⁻³)
2.5 MeV	$Z_{1/2}$	$E_C - 0.68$	1×10^{-14}	a	4.1×10^{13}
	EH5	$E_C - 1.13$	4×10^{-15}	$(1.0 \times 10^{-16})^b$	1.5×10^{13}
	EH6/7	$E_C - 1.51$	1×10^{-14}	$(5.3 \times 10^{-15})^c$	2.1×10^{13}
200 keV	$Z_{1/2}$	$E_C - 0.67$	2×10^{-14}	a	1.2×10^{14}
	EH5 (A)	$E_C - 1.07$	1×10^{-15}	$(1.0 \times 10^{-16})^b$	6.4×10^{13}
	EH5 (B)	$E_C - 1.02$	4×10^{-16}		1.9×10^{13}
	EH6/7	$E_C - 1.57$	4×10^{-14}	$(5.3 \times 10^{-15})^c$	1.6×10^{14}
	EH6/7 (first)	$E_C - 1.67$	2×10^{-13}		1.7×10^{14}

^a (Z_1^- : $1.71 \times 10^{-15} \exp(-0.065 \text{ eV}/k_B T)$ cm²; Z_2^- : $1.31 \times 10^{-15} \exp(-0.080 \text{ eV}/k_B T)$ cm²) Ref. [28]

^b Ref. [18]

^c Ref. [29]

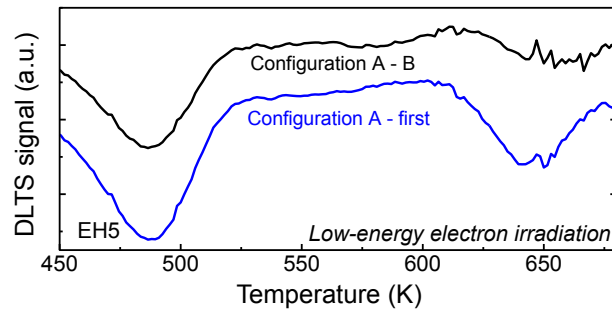


Figure 3. (Color online) Difference spectra of the low-energy electron irradiated 4H-SiC. The defects were stabilized in the two different configurations A and B prior to the DLTS measurement or the first DLTS spectrum after Schottky contact formation was taken into account during subtraction. The difference spectra (configuration A-first and configuration A - B) are shown.

DLTS spectrum is displayed in Figure 2, labeled *first measurement*, which shows the first measurement after Schottky contact formation and CV investigation. Prior to the first measurement, all FB-centers are stable in configuration B. After the first DLTS measurement up to 700 K on a virgin Schottky contact, the EH5 peak may be detected even after annealing without bias. In most instances the transition from configuration A to B is not complete. However, the EH5 peak amplitude can repeatedly be enhanced or decreased depending on the bias conditions at $T \approx 730$ K and thus the FB-center shows a bistable behavior, which is present both after high- and low-energy electron irradiation. Storasta et al. [24] reported that the EH5 peak is not present after low-energy electron irradiation, which agrees partly with our findings of the first measurement after Schottky contact formation.

The fact that the EH5 peak is depending on the bias conditions at temperatures higher than 700 K may explain the interesting properties of this peak published by Alfieri et al. [21, 22]. The authors studied the annealing behavior of defects created after high-energy electron irradiation in 4H-SiC using DLTS measurements. They observed that the EH5 peak is introduced after heat treatments at $T = 573$ K, it increases strongly after annealing at $T = 673$ K before it decreases gradually until its annihilation at about $T = 973$ K. The heat treatments were performed in nitrogen atmosphere. Considering our results, the defect should be in configuration B directly after irradiation and during an up-scan DLTS measurement no EH5 peak should be detected as it was reported. Since Alfieri et al. [21] did their measurements starting from the annealing temperature and varying the temperature downwards, the thermal energy will be enough to transfer parts of the defects from configuration B to configuration A. At higher annealing temperatures, the thermal energy is increased and thus more defects will be transferred to A. That will explain why a maximum EH5 concentration is detected for an annealing temperature $T > 673$ K. For higher temperatures, the defect related to the EH5 peak may start to anneal out.

The difference spectra (configuration A - B and configuration A - first) are shown

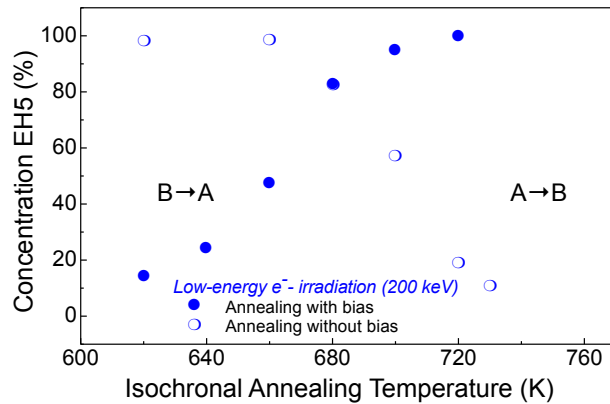


Figure 4. (Color online) Isochronal annealing to study the reconfiguration process of DLTS peak EH5. Defects were prepared initially in configuration A with $V_r = -10$ V (open symbols) and B with $V_r = 0$ V (closed symbols) at $T_{anneal} \geq 730$ K for 15 min and the reconfiguration processes ($A \rightarrow B$ and $B \rightarrow A$) were observed by the EH5 peak amplitude at increasing annealing temperature $t_{anneal}(\text{low-energy}) = 10$ min.

for the low-energy irradiated samples in Figure 3. Additional features occur at the place of the EH6/7 peak. The pronounced peak at about 650 K in the curve *Configuration A - first* shows a metastable behavior for both kinds of samples, the Schottky diodes and the p^+n -junctions. However, the reconfiguration processes ($A \rightarrow B$ and $B \rightarrow A$) occur at similar temperatures which makes it difficult to investigate more detailed its origin, thus further discussions focus on the change in the EH5 peak amplitude. It has to be mentioned that at such high temperatures, the behavior of the Schottky diode may change and thus making it difficult to distinguish from transitions between configurations. However, the investigated p^+n -junctions are more temperature stable and thus strengthening the existence of an additional metastable deep level. Additional to the strange behavior of the EH5 peak, Alfieri et al. [21,22] observed a shift in emission rates of the EH6/7 peak, which is also detected in our samples, see table 1. The EH6/7 peak may change shape because of the superposition with the metastable peak at 650 K.

3.2. Reconfiguration investigations

The DLTS amplitude of the EH5 peak depends on the thermal and electrical history; EH5 is present after cooling with bias and decreased noticeable or is absent after cooling without bias, as explained in section 3.1. The actual reconfiguration temperature was determined by isochronal annealing both for the high- and the low-energy irradiated samples. The defects were stabilized at high temperature in both configurations, cooled down under the chosen bias conditions and the reconfiguration to the opposite configuration was then studied by thermal annealing for a constant annealing time ($t_{anneal}(\text{low-energy}) = 10$ min). It should be noted that the initial B state was very close to the *first measurement*, where no signature of the EH5 peak was detected. The defect concentrations were obtained from the EH5 peak amplitudes subtracting the

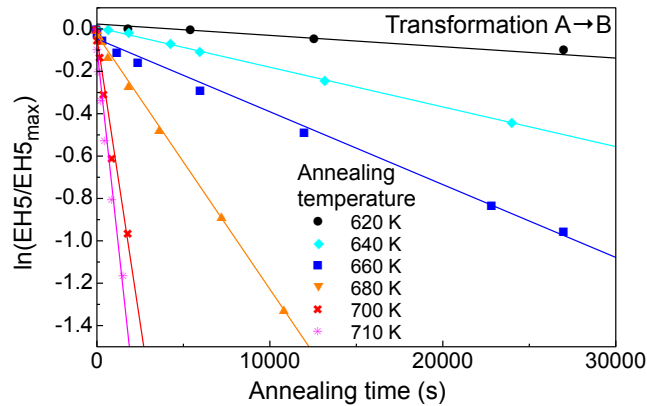


Figure 5. (Color online) Isothermal annealing to determine the reconfiguration energy of DLTS peak EH5. Defects were stabilized in configuration A with $V_r = -10$ V at $T_{anneal} \geq 730$ K for 15 min. The reconfiguration rates were obtained from the decrease of EH5 peak amplitude versus increasing annealing time.

background signal prior the annealing procedure. The determined EH5 concentration versus the annealing temperature is shown in Figure 4 for the samples irradiated with low-energy electrons. More thermal energy is needed to reconfigure from configuration $A \rightarrow B$, than for the transition from $B \rightarrow A$. The threshold temperatures for the corresponding processes ($T_{B \rightarrow A} \approx 710$ K and $T_{A \rightarrow B} > 730$ K) are above 700 K close to the limit of our DLTS setup. The same reconfiguration behavior was observed for high-energy electron irradiated samples, not shown here.

The required thermal energies to change the configuration ($A \rightarrow B$, $B \rightarrow A$) were determined by isothermal annealing by increasing the annealing time, t . The evolution of EH5 amplitude under applied bias during heat treatment, when the defects were prepared initially in B and the decrease of the EH5 signal after stabilizing the defects initially in configuration A were studied.

The reconfiguration rates, $R_{(B \rightarrow A)}$, were determined by fitting the exponential curves using the defect concentration after complete reconfiguration, N_∞ , and the detected defect concentration, N_t , for the distinct temperatures:

$$N_t = N_\infty \{1 - \exp(-R_{(B \rightarrow A)}t)\} \quad (1)$$

For the opposite process ($A \rightarrow B$), the reconfiguration rates, $R_{(A \rightarrow B)}$, were obtained from the linear dependence of the logarithmic of the peak amplitudes on the annealing time shown in Figure 5.

$$N_t = N_\infty \{\exp(-R_{(A \rightarrow B)}t)\} \quad (2)$$

The disappearance of the EH5 signal follows a first order kinetics.

The reconfiguration rates depend exponentially on the inverse temperature.

$$R = R_0 \exp\left(\frac{-E_A}{k_B T}\right) \quad (3)$$

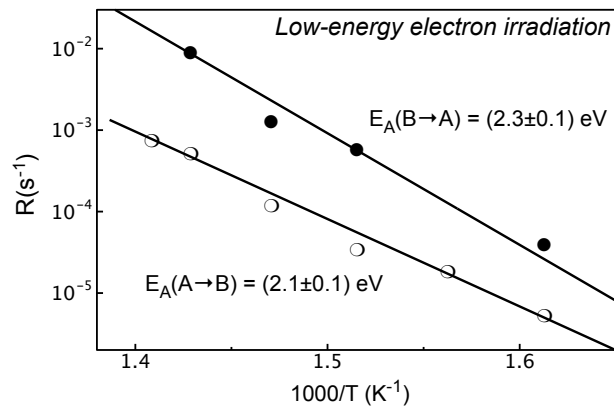


Figure 6. Arrhenius-plot of the reconfiguration rates for the transitions from configuration $A \rightarrow B$ (open symbols) and $B \rightarrow A$ (closed symbols).

The reconfiguration energies were calculated from the slopes of the semi-logarithmic Arrhenius plot in Figure 6 to be $E_A(A \rightarrow B) = (2.1 \pm 0.1)$ eV and $E_A(B \rightarrow A) = (2.3 \pm 0.1)$ eV, respectively. The energy to change the configuration from $B \rightarrow A$ is higher than the opposite process $A \rightarrow B$, even though the reconfiguration temperature suggests the opposite. Important information about the transition process can be obtained from the pre-factor, R_0 , which was $R_0(A \rightarrow B) = 4 \times 10^{11} \text{ s}^{-1}$ and $R_0(B \rightarrow A) = 2 \times 10^{14} \text{ s}^{-1}$, respectively. Pre-factors in the order of 10^{12} s^{-1} , like the one for the transition $A \rightarrow B$, are attributed to an atomic jump process [2]. Thus interaction with the lattice takes place. The pre-factor for the transformation process $B \rightarrow A$ indicates that this transition is dominated by a charge carrier-emission process [2]. The associated electron emission process gives rise to the detected peak EH5.

3.3. Minority charge carrier injection

Besides changing the configuration using thermal energy, the injection of minority charge carriers may also force reconfiguration. In the case of the p^+n junctions the injection is realized by forward biasing the diode. Figure 7 (a) shows the percentage of defects in configuration A. The defects were prepared at high temperature in configuration B and fast cooled down to the EH5 emission temperature ($T = 485$ K) by dipping the sample holder directly into nitrogen. Consequently, the signature of EH5 in the DLTS spectrum should be suppressed. The EH5 amplitude, which is proportional to the concentration of defects in configuration A, increases after a constant injection pulse ($t_{pulse} = 300$ s) with increasing forward current. Using the hole injection pulse, the transition from $B \rightarrow A$ is complete after a forward current of $I > 5 \times 10^{-2}$ A. Minority charge carrier injection forced the transition from configuration B to A, which occurs thermally at much higher temperatures.

Minority charge carrier injection can be realized for majority devices like Schottky diodes by light pulses exceeding the band gap energy of the studied material

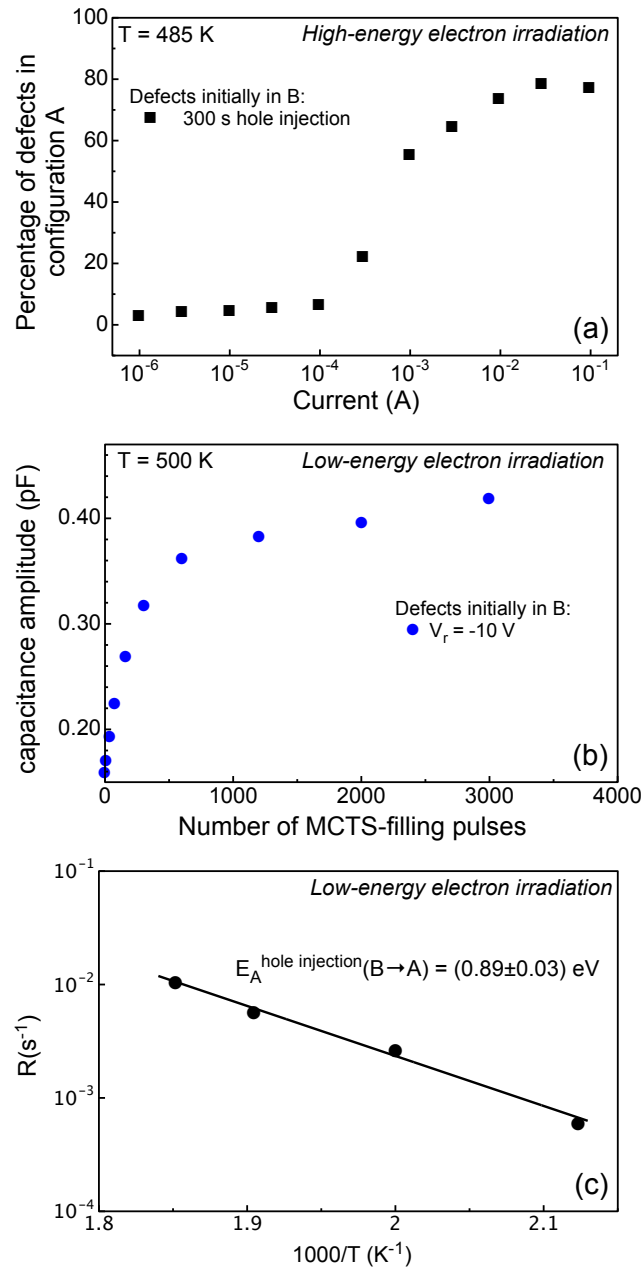


Figure 7. (Color online) Minority charge carrier injection: (a) by forward biasing the p^+n -junction, (b) by the generation of electron-hole pairs through UV-illumination pulses and (c) reconfiguration energy ($B \rightarrow A$) under hole injection.

($E_g(4\text{H-SiC}) = 3.23$) eV [30]). This method, labeled *minority charge carrier transient spectroscopy* (MCTS) is also used to investigate defects located in the lower part of the band gap. The hole concentration will exceed the electron concentration in the depletion region, if the hole diffusion current into the depletion region is larger than the electron drift current out of the depletion region. In Figure 7 (b), the change of the capacitance amplitude close to the emission temperature of EH5 ($T = 500$ K) is shown. If the defects are initialized in configuration B at $T = 730$ K, quickly cooled down to $T = 500$ K with

liquid nitrogen and then exposed to a 1 s long UV-pulse, which generates both electrons and holes, the capacitance amplitude of peak EH5 increases. The defects, which initially were stable in configuration B emit their electrons. The transition from configuration $B \rightarrow A$ is detected. The transition rate increases several orders of magnitudes compared to the extracted thermal reconfiguration rate at 500 K. Determining the transition rates at different temperatures, the reconfiguration energy under hole injection can be obtained as shown in Figure 7 (c). Compared to the thermally induced transition $B \rightarrow A$, the transition $B \rightarrow A$ is facilitated under hole injection and the reconfiguration energy decreases to $E_A^{\text{hole injection}}(B \rightarrow A) = (0.89 \pm 0.03)$ eV. The pre-factor for this transition is $R_0^{\text{hole injection}}(B \rightarrow A) = 2 \times 10^6$ s $^{-1}$ which further strengthens the hole capture process [2].

For both high- and low-energy irradiated samples, hole injection can be used to induce configurational change at lower temperature than the thermal reconfiguration energy allowed. Part of the energy (≈ 1.4 eV) released by the hole capture is added to the thermal energy to overcome the reconfiguration barrier.

3.4. Comparison with metastable defect detected in $6H$ -SiC

It is known, that the valence bands of the different SiC-polytypes [31] align and previously it was observed, that also intrinsic defects align [29, 32]. Hemmingsson et al. [16] detected a multistable defect present in $6H$ -SiC. The electron emission from configuration C1, observed as L1 in the DLTS spectrum in reference [[16]] corresponds perfectly with the emission from the FB-center in configuration A, detected as EH5 peak in the DLTS spectrum. However, the emissions from configuration C2 (DLTS peak: L2) in reference [[16]] and from configuration C3 (DLTS peak: L3) in reference [[16]] were not observed. The DLTS peak expected to be similar to peak L2 will overlap with EH6/7 peak. In the DLTS difference spectrum *configuration A-first* in Figure 3, an additional peak was detected at the position of the EH6/7 peak, which may be connected to a metastable configuration related to the FB-center. The emission energy of L3 is so large, that it will be inaccessible with the existing DLTS setup.

4. Concluding remarks:

After high- and low-energy electron irradiation, the FB-center shows a bistable behavior depending on the thermal, optical and electrical history. Configuration A gives rise to the electron emission associated with DLTS peak EH5. For configuration B, no electron emission related DLTS peak was observed in the accessible temperature range. The transition $A \rightarrow B$ occurs at about 710 K. The opposite transformation $B \rightarrow A$ takes place at such high temperatures $T \approx 730$ K, which are the limits of the DLTS setup, that it may not be completed. However, the first DLTS scan after Schottky contact formation, where no EH5 peak is observed, represents the FB-center fully

transferred to configuration B. Reconfiguration kinetics revealed reconfiguration barriers of: $R_{A \rightarrow B} = 4 \times 10^{11} \exp\{(2.1 \pm 0.1)/(k_B T)\}$ and $R_{B \rightarrow A} = 2 \times 10^{14} \exp\{(2.3 \pm 0.1)/(k_B T)\}$, respectively. The pre-factors suggest an atomic jump for the transformation $A \rightarrow B$ and a charge carrier emission dominated process for the opposite transition $B \rightarrow A$. Both processes are in agreement with the suggested configuration coordinate diagram. Minority charge carrier injection facilitated the transition from configuration B to A. Hole capture reduced the reconfiguration barrier for the transition $B \rightarrow A$ to $E_A^{\text{hole injection}}(B \rightarrow A) = (0.89 \pm 0.03)$ eV. Since the DLTS peak EH5 is detectable after high- and low-energy electron irradiation, the FB-center is likely a carbon related defect.

5. Acknowledgment:

The Swedish Research Council (VR, 2009-3383 and 2008-5243) and the Swedish Energy Agency (P30942-1) are gratefully acknowledged for financial support.

References

- [1] A. Chantre. Configurationally bistable C center in quenched Si:B: Possibility of boron-vacancy pair. *Phys. Rev. B*, 32:3687–3694, 1985.
- [2] A. Chantre. Introduction to Defect Bistability. *Appl. Phys. A*, 48:3–9, 1989.
- [3] C. A. Londos. Electron irradiation-induced defects in p -type silicon at 80 K. *J. Phys. Chem. Solids*, 47:1147 – 1151, 1986.
- [4] L. W. Song, B. W. Benson, and G. D. Watkins. Identification of a bistable defect in silicon: The carbon interstitial-carbon substitutional pair. *Appl. Phys. Lett.*, 51:1155–1157, 1987.
- [5] M. Mamor, M. Willander, F. D. Auret, W. E. Meyer, and E. Sveinbjörnsson. Configurationally metastable defects in irradiated epitaxially grown boron-doped p -type Si. *Phys. Rev. B*, 63:045201, 2000.
- [6] Y. Tokuda. Transformation behavior of room-temperature-stable metastable defects in hydrogen-implanted n -type silicon studied by isothermal deep-level transient spectroscopy. *Journal of Applied Physics*, 100:023704, 2006.
- [7] Yutaka Tokuda and Takeshi Seo. Characterization of a metastable defect labeled EM3 in hydrogen-implanted n -type silicon using deep-level transient spectroscopy. *J. Mater. Sci.: Mater. Electron.*, 19:281–284, 2008.
- [8] F. D. Auret, R. M. Erasmus, and S. A. Goodman. A Metastable Alpha-Particle Irradiation Induced Defect in n -GaAs. *Jpn. J. Appl. Phys.*, 33:L491–L493, 1994.
- [9] M. J. Legodi, F. D. Auret, and S. A. Goodman. Electronic and transformation properties of a metastable defect introduced in epitaxially grown sulfur doped n -GaAs by particle irradiation. *Mater. Sci. Eng. B*, 71:96 – 99, 2000.
- [10] M. Levinson. Capacitance transient analysis of configurationally bistable defects in semiconductors. *J. Appl. Phys.*, 58:2628–2633, 1985.
- [11] V.V. Peshev. A bistable defect in InP. *Russ. Phys. J.*, 48:417–422, 2005.
- [12] D. M. Martin, H. Kortegaard Nielsen, P. Lévêque, A. Hallén, G. Alfieri, and B. G. Svensson. Bistable defect in mega-electron-volt proton implanted $4H$ silicon carbide. *Appl. Phys. Lett.*, 84:1704–1706, 2004.
- [13] H. K. Nielsen, A. Hallén, and B. G. Svensson. Capacitance transient study of the metastable M center in n -type $4H$ – SiC. *Phys. Rev. B*, 72:085208, 2005.

- [14] F. C. Beyer, C. G. Hemmingsson, H. Pedersen, A. Henry, J. Isoya, N. Morishita, T. Ohshima, and E. Janzén. Bistable defects in low-energy electron irradiated n-type 4H-SiC. *Phys. Status Solidi Rap. Res. Lett.*, 4:227–229, 2010.
- [15] F. C. Beyer, C. Hemmingsson, H. Pedersen, A. Henry, E. Janzén, J. Isoya, N. Morishita, and T. Ohshima. Annealing behavior of the EB-centers and M-center in low-energy electron irradiated n-type 4H-SiC. *J. Appl. Phys.*, 109:103703, 2011.
- [16] C. G. Hemmingsson, N. T. Son, O. Kordina, and E. Janzén. Metastable defects in 6H-SiC: experiments and modeling. *J. Appl. Phys.*, 91:1324–1330, 2002.
- [17] H. J. von Bardeleben, J. L. Cantin, L. Henry, and M. F. Barthe. Vacancy defects in p-type 6H-SiC created by low-energy electron irradiation. *Phys. Rev. B*, 62:10841–10846, 2000.
- [18] C. Hemmingsson, N. T. Son, O. Kordina, J. P. Bergman, E. Janzén, J. L. Lindström, S. Savage, and N. Nordell. Deep level defects in electron-irradiated 4H SiC epitaxial layers. *J. Appl. Phys.*, 81:6155–6159, 1997.
- [19] M. L. David, G. Alfieri, E. M. Monakhov, A. Hallén, C. Blanchard, B. G. Svensson, and J. F. Barbot. Electrically active defects in irradiated 4H-SiC. *J. Appl. Phys.*, 95:4728–4733, 2004.
- [20] A. Castaldini, A. Cavallini, L. Rigutti, and F. Nava. Low temperature annealing of electron irradiation induced defects in 4H-SiC. *Appl. Phys. Lett.*, 85:3780–3782, 2004.
- [21] G. Alfieri, E. V. Monakhov, B. G. Svensson, and A. Hallén. Defect energy levels in hydrogen-implanted and electron-irradiated n-type 4H silicon carbide. *J. Appl. Phys.*, 98:113524, 2005.
- [22] G. Alfieri, E. V. Monakhov, B. G. Svensson, and M. K. Linnarsson. Annealing behavior between room temperature and 2000 °C of deep level defects in electron-irradiated n-type 4H silicon carbide. *J. Appl. Phys.*, 98:043518, 2005.
- [23] A. Castaldini, A. Cavallini, L. Rigutti, S. Pizzini, A. Le Donne, and S. Binetti. Diffusion length and junction spectroscopy analysis of low-temperature annealing of electron irradiation-induced deep levels in 4H-SiC. *J. Appl. Phys.*, 99:033701, 2006.
- [24] L. Storasta, J. P. Bergman, E. Janzén, A. Henry, and J. Lu. Deep levels created by low energy electron irradiation in 4H-SiC. *J. Appl. Phys.*, 96:4909–4915, 2004.
- [25] L. Storasta, F. H. C. Carlsson, J. P. Bergman, and E. Janzén. Observation of recombination enhanced defect annealing in 4H-SiC. *Appl. Phys. Lett.*, 86:091903, 2005.
- [26] K. Danno and T. Kimoto. Investigation of deep levels in n-type 4H-SiC epilayers irradiated with low-energy electrons. *J. Appl. Phys.*, 100:113728, 2006.
- [27] T. Dalibor, G. Pensl, H. Matsunami, T. Kimoto, W. J. Choyke, A. Schöner, and N. Nordell. Deep Defect Centers in Silicon Carbide Monitored with Deep Level Transient Spectroscopy. *Phys. Stat. Solidi A*, 162:199–225, 1997.
- [28] C. G. Hemmingsson, N. T. Son, A. Ellison, J. Zhang, and E. Janzén. Negative-U centers in 4H silicon carbide. *Phys. Rev. B*, 58:R10119–R10122, 1998.
- [29] F. C. Beyer, C. G. Hemmingsson, A. Gällström, S. Leone, H. Pedersen, A. Henry, and E. Janzén. Deep levels in tungsten doped n-type 3C-SiC. *Appl. Phys. Lett.*, 98:152104, 2011.
- [30] Y. Goldberg, M.E. Levinshtein, and S.L. Rumyantsev. *Properties of Advanced Semiconductor Materials: GaN, AlN, SiC, BN, SiC, SiGe*. John Wiley & Sons, Inc., New York, 2001.
- [31] V. V. Afanas'ev, M. Bassler, G. Pensl, M. J. Schulz, and E. Stein von Kamienski. Band offsets and electronic structure of SiC/SiO₂ interfaces. *J. Appl. Phys.*, 79:3108–3114, 1996.
- [32] S. Sasaki, K. Kawahara, G. Feng, G. Alfieri, and T. Kimoto. Major deep levels with the same microstructures observed in n-type 4H-SiC and 6H-SiC. *J. Appl. Phys.*, 109:013705, 2011.